Atom-surface scattering under classical conditions

André Muis and J. R. Manson

Department of Physics and Astronomy, Clemson University, Clemson, South Carolina 29634

(Received 4 December 1995)

Classical limit expressions of the differential reflection coefficient for atomiclike projectiles scattering from a surface are compared with recent experiments for the scattering of 200-eV Na$^+$ ions from Cu(001). Good agreement with the experiment and with previous theoretical calculations for the temperature dependence of the peak widths is obtained. The calculations suggest that further comparisons with the scattered lobes will produce important information about the projectile interaction and about vibrational correlations at the surface. [S0163-1829(96)06124-3]

The surface scattering of atomic projectiles under quantum mechanical conditions, and particularly the scattering of He, is an experimental tool that has produced extensive information on surface dynamics and on the atom-surface interaction.[1,2] Far fewer experiments have been carried out under the classical conditions for vibrational energy transfer, which consist of large projectile masses, high incident energies, and large surface temperatures.[3–6] Under such conditions the scattering problem becomes very complex and involves the exchange of many phonon quanta. Additionally, at high energies thresholds for the appearance of new quantum processes are crossed and such events as atomic electronic excitations of either the projectile or the crystal cores become possible. An understanding of energy and momentum exchange in the classical regime is very important for establishing the interaction potentials and the crystal dynamics at these energies, and is also necessary for an understanding of macroscopic physical processes at gas-surface interfaces such as energy accommodation, sticking, and drag and lift forces.

Recently, a very interesting classical regime experiment has been reported for high-resolution, energy-resolved scattering intensities of Na$^+$ ions with energies of several hundred eV from a Cu(001) surface.[7] Of the several features observed in the spectra, one was identified as a peak due to single-scattering events, and the widths of this peak as a function of temperature and polar scattering angle were explained quite well with recently developed semiclassical scattering theories taken in the classical limit.[8,9] Under the conditions of this experiment, approximately half or more of the incident Na$^+$ translational kinetic energy was deposited in the crystal surface by the projectiles in the backscattered intensity. Theoretical comparisons were also made with the semiclassical trajectory approximation (TA) and this approximation was found to fail completely for these high translational energy-loss experiments.

The purpose of this paper is to compare these recent measurements with the complete classical theory for the scattering intensity, which is obtained from the quantum multiphonon calculations in the correspondence limit. In addition to reproducing the global width features of the measured intensities, this theory makes predictions of the angular and energy-dependent shapes of the scattered intensity lobes, which indicate that further comparison with experiment can give important information on surface interactions and vibrational correlations.

Most quantum mechanical treatments of the inelastic exchange of vibrational energy in atom-surface collisions begin by describing the system in terms of a Hamiltonian of the form

$$H = H_0^c + H_0^p + V, \tag{1}$$

where H_0^c is the unperturbed crystal Hamiltonian, H_0^p is the unperturbed Hamiltonian of the projectile, and V is the interaction potential coupling the two. The potential V is then expanded in terms of the small crystal displacements

$$V = V_0 + V_1 + \cdots . \tag{2}$$

The zeroth-order term describes purely elastic scattering, and the first order term is linear in the crystal displacements. Neglecting higher-order terms in the displacement leaves the problem in the form of a general linear forced oscillator. Higher-order terms in Eq. (2) become unimportant in the classical limit[10–13] and they have also been shown to be of little importance even for typical He-scattering systems at low energies.[14]

The classical scattering limit for such a system can be obtained in the correspondence limit of large numbers of quanta transferred, and is effectively independent of the vibrational spectrum of the surface. The essential approximations necessary for passing to the classical limit are as follows: (1) to retain only classically allowed trajectories; (2) the collision time is taken to be short compared to all phonon vibrational periods of the crystal (which implicitly requires initial and final projectile energies much greater than $k_B \Theta_D$, where Θ_D is the Debye temperature and k_B is Boltzmann's constant); and (3) in order to eliminate quantum effects of the crystal motion, $T_S \gg \Theta_D$, where T_S is the surface temperature. (In actual practice this latter condition is almost always satisfied if $T_S > \Theta_D/2$.) This third condition is not necessary for obtaining a closed-form solution, and in fact low-temperature quantum behavior of the lattice can be readily included and is in principle observable in the peak intensities and widths as $T_S \to 0$ even with high-energy projectiles.[8,15]

There are two distinct limiting cases for classical scattering: scattering from a surface of discrete scattering centers or from a continuum surface. For scattering from a surface made up of a collection of discrete scattering centers the result, as expressed in terms of the experimentally measurable differential reflection coefficient, has the following form:[10,13]

$$\frac{dR}{d\Omega_f dE_f} = \frac{m^2 |\mathbf{p}_f|}{8\pi^3 \hbar^4 p_{iz}} |\tau_{fi}|^2 \left(\frac{\pi}{\Delta E_0 k_B T_S}\right)^{1/2}$$

$$\times \exp\left\{-\frac{(\Delta E + \Delta E_0)^2}{4 k_B T_S \Delta E_0}\right\}, \quad (3)$$

where $\Delta E = E_f^p - E_i^p$ is the difference between the final and initial projectile energies, the momentum $\mathbf{p}_q$ of a particle in state q is divided into components parallel and perpendicular to the surface, respectively, according to $\mathbf{p}_q = (\mathbf{P}_q, p_{qz})$, $|\tau_{fi}|^2$ is the scattering form factor of a unit cell, and m is the atomic mass. $\Delta E_0 = (\mathbf{p}_f - \mathbf{p}_i)^2 / 2M_c$, where M_c is the crystal mass, is the recoil energy shift, arising from the quantum mechanical zero-point motion. Although Eq. (3) appears Gaussian-like in $\Delta E + \Delta E_0$, the energy dependence of ΔE_0 can give rise to highly asymmetric peak shapes, for example, under conditions in which $E_f^p \gg E_i^p$.[16]

In the limiting case of classical scattering from a continuum surface the differential reflection coefficient takes on the slightly more complicated form:[11,12,17,18]

$$\frac{dR}{d\Omega_f dE_f} = \frac{m^2 v_R^2 |\mathbf{p}_f|}{4\pi^3 \hbar^2 p_{iz} S_{uc}} |\tau_{fi}|^2 \left(\frac{\pi}{\Delta E_0 k_B T_S}\right)^{3/2}$$

$$\times \exp\left\{-\frac{(\Delta E + \Delta E_0)^2 + 2 v_R^2 \mathbf{P}^2}{4 k_B T_S \Delta E_0}\right\}, \quad (4)$$

where $\mathbf{P}$ is the parallel momentum exchange $\mathbf{P} = \mathbf{P}_f - \mathbf{P}_i$, S_{uc} is the area of a surface unit cell, and v_R is a weighted average of sound velocities parallel to the surface[11] and the term in the Gaussian-like exponent involving v_R arises from scattering from vibrational correlations at the surface.

Both Eqs. (3) and (4) are descriptions in the recoil limit, in which the energy exchange is mechanical and due to recoil of the surface. Relaxation of the recoil energy of the surface atoms into the crystal phonon field occurs only after the collision is finished. Hence the surface temperature dependence in Eqs. (3) and (4) arises solely from the mean square displacement of the surface before the collision. This holds true even for temperatures sufficiently high that surface anharmonicity is induced, in which case T_S would be replaced by a power series in T_S beginning with the linear term.

It is interesting to note that Eqs. (3) and (4) are derived from trajectory calculations, which is an inherent property of all classical calculations, but they use trajectories beginning with the projectile initially having momentum $\mathbf{p}_i$ and after collision ending in momentum $\mathbf{p}_f$, and the recoil energy is correctly calculated. This marks the distinction with the usual semiclassical TA in which the recoil energy is taken to be independent of the final energy. Thus at high incident energies and for comparably sized projectile and target masses where the recoil can be significant, the TA can produce very poor estimates for ΔE_0 and can lead to results quite different from those of the exact classical expressions.
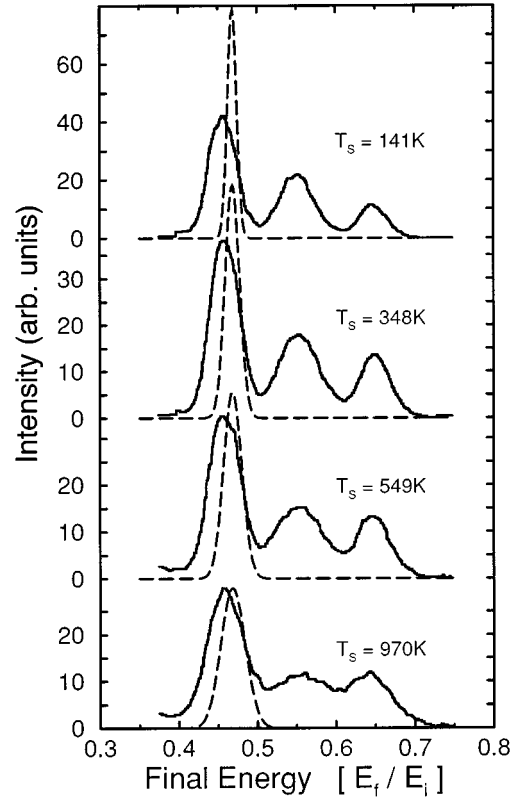
FIG. 1. Energy-resolved intensity spectra plotted as a function of final particle energy for 201.2-eV Na$^+$ scattered from Cu(001)$\langle 100 \rangle$ for four different surface temperatures with $\theta_i = \theta_f = 45°$. The solid lines are the experimental measurements (Ref. 7) and the dashed lines are the calculations of Eq. (3).

Figure 1 shows a set of measured energy-resolved intensity spectra taken at four different surface temperatures for 201-eV Na$^+$ incident at $\theta_i = \theta_f = 45°$ on Cu(001)$\langle 100 \rangle$.[7] Three distinct peaks are observed in each of the spectra; the peak at the smallest value of E_f^p is due to single scattering of the Na with the surface and is the peak of interest here. The two smaller peaks at larger E_f^p have been identified as arising from multiple scattering,[7,19] and are not of interest for the present considerations. The dashed lines in Fig. 1 are the calculations of Eq. (3), and the agreement with the data is surprisingly good for a theory with no adjustable parameters. The calculated peak positions agree with the measured positions to within 4% and the calculated widths, although smaller than the measured widths, show a similar increase with T_S.

The calculated peak position is very nearly given by the zero of the argument of the exponential in Eq. (3), $E_f^p = E_i^p - \Delta E_0$. This is the classical recoil expression, which assumes that the impulse momentum is deposited in a single-crystal atom and can be expressed in terms of the total scattering angle $\theta = \pi - \theta_f - \theta_i$ and the reduced mass $\mu = m/M_c$, as $E_f^p = f(\theta) E_i^p$, where

$$f(\theta) = \left(\frac{\sqrt{1 - \mu^2 \sin^2\theta} + \mu \cos\theta}{1 + \mu}\right)^2. \quad (5)$$

This equation shows that the peak position is very sensitive to both projectile and surface mass, even to the extent of

being isotope dependent, e.g., a change of the mass of either Cu or Na by 1 amu will cause a 1% or 3% shift in the calculated peak positions, respectively.

The form factor was chosen as a constant, implying uniform weighting in all directions. However, at these high energies the calculations do not make an appreciable distinction between, for example, a constant form factor and the semiclassical hard wall limit given by $\tau_{fi} = 2p_{fz}p_{iz}/m$. Similarly, often important questions in other time-of-flight experiments such as the difference between intensities measured by a density or a flux detector, namely, a factor of p_f, do not have an appreciable effect at these energies.

The widths of the calculated peaks increase with T_S as do the measured widths, but at all temperatures the measured widths are larger by the same constant value. It is immediately evident from Eq. (4) that the width of the differential reflection coefficient will be very nearly proportional to $\sqrt{T_S}$. In Ref. 7, careful measurements were made of the widths between $T_S = 141$ and 970 K and, expressed in terms of the second moment of the intensity about the mean $\langle \Delta E^2 \rangle$, they were very closely fitted by the linear function $\langle \Delta E^2 \rangle = A + 2g(\pi - \theta_i - \theta_f)E_i^p k_B T_S$ with $A \approx 8$ eV^2 and $g(\pi/2) = 0.291 \pm 0.020$ for $\theta_f = 45°$. Reference 7 also measured the slope $g(\theta)$ as a function of final scattered angle θ_f for the same fixed initial conditions ($\theta_i = 45°$ and $E_i^p = 201.2$ eV) as in Fig. 1. Their theoretical calculations for $\langle \Delta E^2 \rangle$ do not predict the temperature-independent part of the width; however, they agree quite well with the measured slope $g(\theta)$. Equation (3) produces identical results for the calculated widths.

Clearly the temperature and angular dependence of the peak widths are well explained by the parameter free theory, either by the expression of Eq. (3) above or by the classical theory utilized in Ref. 7. However, it is of interest to examine whether Eq. (4) gives a better description than Eq. (3) for this system. Equation (3) is clearly appropriate for projectiles that interact weakly with the crystal atom cores, such as in neutron scattering,[10] and the intensity given by Eq. (3) appears mostly in the forward direction. Equation (4), on the other hand, because of the additional dependence on the parallel momentum transfer caused by the repulsive surface, gives well-defined lobes backscattered above the surface. Equation (4) has been demonstrated to be the correct form for He scattering at incident energies below 1 eV through direct measurements of the characteristic $T_S^{-3/2}$ temperature dependence of the maximum multiphonon peak intensity.[20]

Figure 2 shows the same results as Fig. 1 except that now the calculations are done with Eq. (4). The average surface phonon velocity parameter was chosen as $v_R = 1700$ m/s in rough agreement with the measured Rayleigh wave velocity for Cu(001) of 1500 m/s in the $\langle 100 \rangle$ azimuth and 1800 m/s in the $\langle 110 \rangle$.[21] The calculated peak positions and widths are very nearly identical to those given by Eq. (3) in Fig. 1.

The calculated peak positions and the widths as measured by $g(\theta)$ are essentially identical with the previously mentioned calculations for Eq. (3), and are very nearly independent of v_R for $v_R \lesssim 5000$ m/s, while for $v_R > 5000$ m/s the slopes are somewhat reduced at larger θ_f. The relative intensities of Eq. (4) depend on v_R.

The major difference between the two theoretical expressions is that Eq. (3) implies that the majority of the incident
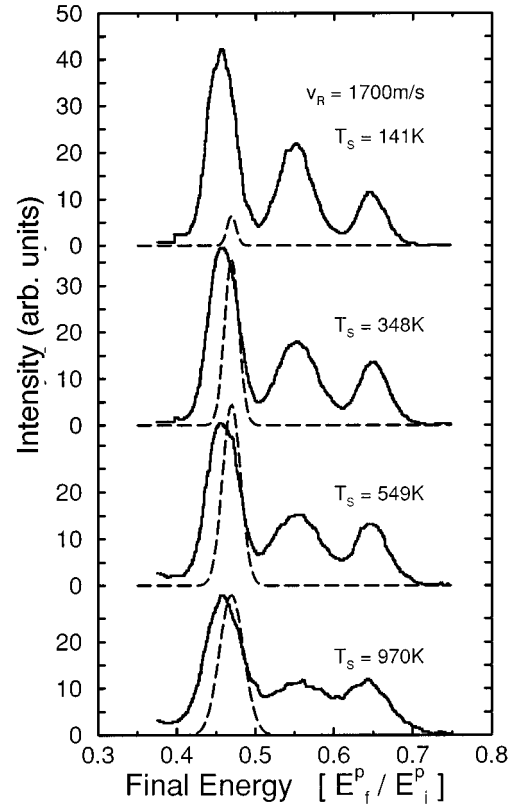
FIG. 2. Energy-resolved intensity spectra as in Fig. 1 for 201.2-eV Na$^+$ scattered from Cu(001)$\langle 100 \rangle$ for four different surface temperatures with $\theta_i = \theta_f = 45°$. The solid lines are the experimental measurements and the dashed lines are the calculations of the continuum model of Eq. (4).

projectiles penetrate the crystal, while Eq. (4) gives well-defined backscattered lobes. This behavior is shown in Fig. 3, which gives the integral of the differential reflection coefficient over all final energies, $dR/d\Omega_f$, plotted as a function of θ_f in a polar graph. The solid line curve shows the relative
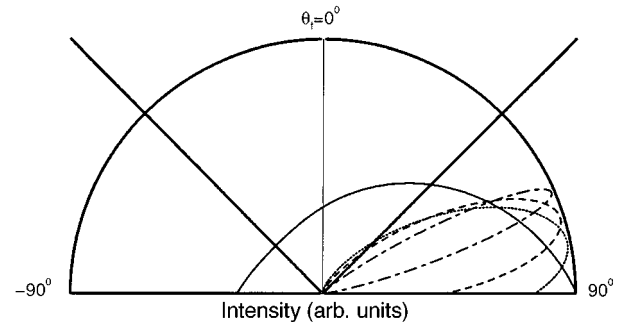
FIG. 3. Energy-integrated angular intensities $dR/d\Omega_f$ plotted as a function of θ_f in a polar plot for the single-scattering peak at $T_S = 970$ K of Fig. 1: The solid line denotes results of the discrete model of Eq. (3). The other calculations are for the continuum model of Eq. (4) with different values of v_R: dotted line, $v_R = 1300$ m/s; dashed line, $v_R = 1700$ m/s; and dash-dotted line, $v_R = 4000$ m/s. The straight lines are the incident and specular directions at $\pm 45°$.

backscattered intensity predicted by Eq. (3) and the other curves show the lobes predicted by Eq. (4) for the three values of $v_R = 1300$, 1700, and 4000 m/s, all for the same temperature $T_S = 970$ K. The lobes produced by Eq. (4) give the majority of the intensity at supraspecular angles, and the lobes move toward the specular direction and become narrow as a function of increasing v_R. In fact, in the limit of $v_R \to \infty$ one obtains the hard cubes condition of zero parallel momentum transfer, i.e., $\mathbf{P}_f = \mathbf{P}_i$. This graph also indicates that for $\theta_i = 45°$ the majority of particles are scattered at angles greater than 60°, and hence the best place to measure the temperature dependence of the energy resolved spectra may be at angles θ_f near the expected maximum of the single scattering lobe. The geometry exhibited in Fig. 3 shows that the measurements were taken at the extreme upper edge of the predicted single-scattering lobe for $v_R = 1700$ m/s. This explains why the maximum intensities calculated in Fig. 2 do not follow the $T_S^{-3/2}$ dependence of the envelope function of Eq. (4); because of the narrowing of the lobes with decreasing T_S, the fixed $\theta_f = 45°$ measuring angle intersects the lobe at a position of smaller inelastic intensity at low T_S.

We have shown that well-known classical-limit expressions for the scattered intensity agree quite well with the temperature and angular dependence of the widths of the measured scattered peaks of Na$^+$ bombarding a Cu(001) surface. These analytic and closed-form classical expressions are also in agreement with the mean square energy moments calculated independently from the energy-projected classical probabilities.[8]

Interestingly, the classical theory with no free parameters predicts very well the temperature dependence of the widths of the measured single-scattering intensity peaks, but does not explain the additional temperature-independent constant width A. One would expect that for a high-energy charged projectile such as Na$^+$ there would be considerable excitation of low-energy electron-hole pairs in the conduction electron sea,[22] although the debate over electron-hole pair production is far from being completely clear.[23,24] However, the complete determination of the temperature dependence of the widths by simple mechanical recoil energy exchange at the surface argues against appreciable direct creation of low-energy electron-hole pairs, because thermal excitation of these additional elementary excitations would contribute additional temperature dependence in the scattered intensities that is not observed. The lack of evidence for direct low-energy electron-hole pair creation is consistent with the classical interpretation given by both Eqs. (3) and (4) and that of Ref. 8 in which the energy exchange is dominated by the initial recoil of the surface atomic cores. Only after the collision, when the backscattered projectiles have left the surface region, does this recoil energy dissipate into the lattice. The dissipation of the recoil energy goes into both phonon creation and electron-hole pair excitation, but the relative proportions appear to be unmeasurable by this experiment.

Some of the constant, temperature-independent term in the measured width, which was not correctly predicted by the classical theory, may be due to experimental uncertainty in energy and angular broadening,[7] but additional broadening on the energy-loss side could come from direct atomic electronic excitations including high-energy electron-hole pair creation in the core levels, and from surface plasmon creation. High-energy atomic excitations are known to be directly created in ion-surface collisions in this energy range,[19,25,26] and this explanation is certainly consistent with Figs. 1 and 2, as the additional constant width of the single-scattering peak is seen to lie always on the energy-loss side of the calculated intensity.

The present calculations using the complete classical differential reflection coefficients reaffirm and add additional explanation to the previous conclusion of Ref. 7 that the semiclassical trajectory approximation is inadequate for large projectile masses and high energies where the kinetic energy loss of the projectile to the surface is significant. These calculations suggest that measurements of scattered angular lobes of the single-scattering peak of Fig. 1 would be sufficient to distinguish between the applicability of Eq. (3) or (4). Such measurements would indicate the effects of correlated surface motion through the measured value of the single parameter v_R. The applicability of Eq. (3) or (4) can also be checked through comparisons with measurements of the maximum peak intensity of the energy resolved differential reflection coefficient for the single-scattering peak as a function of surface temperature, as the two equations have envelope functions that give a readily distinguishable difference in behavior.

---

[1] *Helium Atom Scattering*, Springer Series in Surface Sciences Vol. 27, edited by E. Hulpke (Springer-Verlag, Heidelberg, 1992); J. P. Toennies, in *Surface Phonons*, edited by W. Kress and F. W. de Wette, Springer Series in Surface Sciences Vol. 21 (Springer-Verlag, Heidelberg, 1991), p. 111.

[2] V. Bortolani and A. C. Levi, Revista Nuovo Cimento **9**, 1 (1986).

[3] J. E. Hurst, L. Wharton, K. C. Janda, and D. J. Auerbach, J. Chem. Phys. **78**, 1559 (1983).

[4] E. Hulpke, Surf. Sci. **52**, 615 (1975); U. Gerlach-Meyer and E. Hulpke, Chem. Phys. **22**, 325 (1977).

[5] H. F. Winters, H. Coufal, C. T. Rettner, and D. S. Bethune, Phys. Rev. B **41**, 6240 (1990).

[6] A. Amirav and M. J. Cardillo, Phys. Rev. Lett. **57**, 2299 (1986).

[7] C. A. DiRubio, D. M. Goodstein, B. H. Cooper, and K. Burke, Phys. Rev. Lett. **73**, 2768 (1994).

[8] K. Burke, J. H. Jensen, and W. Kohn, Surf. Sci. **241**, 2771 (1991).

[9] D. M. Goodstein, C. A. DiRubio, B. H. Cooper, and K. Burke (unpublished).

[10] A. Sjölander, Ark. Fys. **14**, 315 (1959).

[11] R. Brako and D. M. Newns, Phys. Rev. Lett. **48**, 1859 (1982); Surf. Sci. **123**, 439 (1982).

[12] H.-D. Meyer and R. D. Levine, Chem. Phys. **85**, 189 (1984).

[13] D. A. Micha, J. Chem. Phys. **74**, 2054 (1981).

[14] G. Armand, J. R. Manson, and C. S. Jayanthi, J. Phys. (Paris) **47**, 1357 (1986); J. R. Manson and G. Armand, Surf. Sci. **195**, 513 (1988).

[15] J. R. Manson, J. Phys. Condens. Matter **5**, A283 (1993).

[16] J. R. Manson and J. G. Skofronick, Phys. Rev. B **47**, 12 890 (1993).

[17] J. R. Manson, Phys. Rev. B **43**, 6924 (1991).

[18] J. R. Manson, Comput. Phys. Commun. **80**, 145 (1994).

[19] J. B. Marston, D. R. Andersson, E. R. Behringer, B. H. Cooper, C. A. DiRubio, G. A. Kimmel, and C. Richardson, Phys. Rev. B **48**, 7809 (1993).

[20] F. Hofmann, J. P. Toennies, and J. R. Manson, Surf. Sci. **349**, L184 (1996).

[21] J. Ellis, N. S. Luo, A. Reichmuth, P. Ruggerone, J. P. Toennies, and G. Benedek, Phys. Rev. B **48**, 4917 (1993).

[22] O. Gunnarson and K. Schönheimer, Phys. Rev. B **25**, 2514 (1982).

[23] R. Brako and D. M. Newns, Surf. Sci. **108**, 42 (1981); Rep. Prog. Phys. **52**, 655 (1989).

[24] Z. Criljen and B. Gumhalter, Surf. Sci. **117**, 116 (1982); **126**, 666 (1983); **139**, 231 (1984); Phys. Rev. B **29**, 6600 (1984).

[25] M. H. Shapiro and Joseph Fine, Nucl. Instrum. Methods Phys. Res. B **44**, 43 (1989).

[26] M. H. Shapiro, T. Tombrello, and J. Fine, Nucl. Instrum. Methods Phys. Res. B **74**, 385 (1993).